

Results from the Pierre Auger Observatory

IOANA C. MARIȘ for the PIERRE AUGER COLLABORATION

Laboratoire de physique nucléaire et des hautes énergies - Paris, France

(ricevuto il 14 Settembre 2010; pubblicato online l'11 Gennaio 2011)

Summary. — Ultra high energy cosmic rays are observed at the Pierre Auger Observatory, the largest cosmic rays experiment in operation, through a hybrid technique employing fluorescence and surface detectors. We present the measurements on the evolution of the mass with energy, the energy spectrum features, photon and neutrino limits and anisotropies based on the data collected between 2004 and 2009.

PACS 98.70.Sa – Cosmic rays (including sources, origin, acceleration, and interactions).

PACS 95.55.Vj – Neutrino, muon, pion, and other elementary particle detectors; cosmic ray detectors.

1. – Introduction

The identification of the origin of the highest energy particles relies on the knowledge of the propagation in the magnetic fields, of the space distributions of sources and on their predicted fluxes. The determination of the energy, the mass and the arrival directions of the ultra high energy cosmic rays is an essential element to solve this inquiry. The Pierre Auger Observatory has delivered, even during its construction stage, accurate measurements of the spectral features, evidence for anisotropies at the highest energies, the most stringent limits on the neutrino and photon fluxes and a precise measurement of the evolution of the mass composition with energy.

At the highest energies a flux suppression is present and can be attributed to the interaction of the cosmic rays with the cosmic microwave background (CMB), the Greisen-Zatsepin-Kuz'min (GZK) effect [1, 2], or to the maximum acceleration power of the sources. The ankle, a hardening of the energy spectrum measured at around 3 EeV, can originate from either the transition from the galactic to the extragalactic components or from the e^\pm production of protons interacting with the CMB [3]. These models cannot be distinguished from the spectral shape, but both differ by the mass composition of the cosmic rays that reach the Earth and their anisotropy properties.

The hadronic cosmic rays are accompanied by photons and neutrinos produced at the acceleration sites and during the propagation of protons. The current limits on high energy neutrinos and photons fluxes are excluding the top-down production scenarios, but are still far from predicted GZK flux.

2. – Pierre Auger Observatory

Cosmic rays, entering the atmosphere interact with the air and produce extensive air showers. The Pierre Auger Observatory [4], located in the province of Mendoza (Argentina), is used to measure the properties of extensive air showers by observing their longitudinal development in the atmosphere as well as their lateral spread at ground level. The charged particles that reach the ground are detected with the surface detector (SD), their lateral extension at cosmic rays energies above 10^{18} eV is of the order of a few kilometers. The Observatory contains more than 1600 independent water-Cerenkov detectors, filled with 12 tons of water each and equipped with three photomultipliers to detect secondary photons and charged particles. The tanks are spread over about 3000 km^2 on a triangular grid of 1.5 km spacing.

On the way through the atmosphere charged particles excite nitrogen molecules, which afterwards emit fluorescence light in the ultra-violet band. The amount of light is proportional to the energy deposited by the air shower. The atmosphere above the surface detector is viewed by four fluorescence detectors (FD), each housing six telescopes, located on the border of the area. The field of view of each telescope is 30° in azimuth, and $1.5\text{--}30^\circ$ in elevation. Light is focused with a spherical mirror of 11 m^2 effective area on a camera of 440 hexagonal pixels.

More details on detector setup and calibration can be found in [4, 5]. An extension of the Observatory [6] has been started with AMIGA [7], a denser array of tanks equipped with muon counters which will lower the trigger threshold energy for the SD, HEAT, three telescopes that will increase the field of view of FD up to 60° and AERA a 20 km^2 antenna array to detect the radio signal produced in air showers by e^\pm interactions with the geomagnetic field. The counterpart of the Southern side is in the planning phase in the Northern hemisphere, in Lamar, Colorado and will be built to provide large statistics above 50 EeV.

An example of a reconstruction of the same air shower with the SD and FD is shown in fig. 1. The signals recorded in the tanks are expressed in terms of vertical equivalent muons (VEM), the average of the signals produced in the 3 PMTs by a vertical muon that passes centrally through the detector. The air shower axis, in case of the SD reconstruction, is obtained from the arrival time of the first particles in each surface detector. The angular resolution is better than 1 degree for events that triggered more than 6 stations. The impact point on the ground and the lateral distribution of signals are obtained in a global likelihood maximization which accounts for the station trigger threshold and the overflow of the FADCs counts in the stations very close to the shower axis. The fluctuations of the lateral distribution function, influenced by the array spacing, are minimized at 1000 m. The signal at this specific distance, $S(1000)$, is corrected through a constant intensity method for the attenuation in the atmosphere and then is used as the energy estimator.

About one in ten air showers that reach the surface detector are also observed with the fluorescence detector which operates only on moonless clear nights. The longitudinal profile of the air shower, *i.e.* the energy deposit as a function of traversed matter in the atmosphere, is obtained from fluorescence and Cerenkov light taking into account the

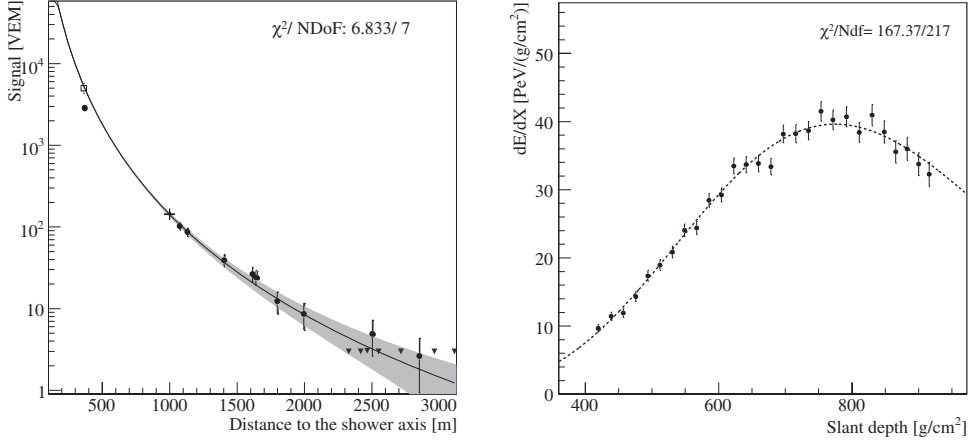


Fig. 1. – A typical golden hybrid event reconstruction, with an energy of 30 EeV and an incoming direction of 27° . Left-hand side: lateral distribution. Filled circles represent acquired signals, triangles are functioning stations without signal used with Poisson probabilities in the maximum likelihood fit. $S(1000)$ is marked with a cross. Right-hand side: longitudinal profile: energy deposit in the atmosphere as a function of the slant depth.

light scattering and attenuation [8]. The energy of the cosmic ray is the integral over the entire longitudinal profile with a correction for the energy carried away by the neutrinos and muons which cannot be seen by FD.

The hybrid reconstruction of events employs, besides the information from the cameras, the timing information of one surface detector, resulting in a good angular and energy resolutions. The energy resolution for the hybrid events is 6% above 1 EeV, while the angular resolution is 0.6 degree.

The energy calibration of the surface detector data is obtained from the events that have been recorded and reconstructed with both SD and FD. The $S(1000)$ shows a power law dependence on the primary energy. The resolution of the energy obtained from $S(1000)$ is energy dependent and varies from 17% at 3 EeV to about 7% at the highest energies.

3. – The flux and the arrival directions

The only quality criteria applied on the surface detector data used for the energy spectrum is that the station with the highest signal is surrounded by 6 active stations. This leads to a simple calculation of the exposure for the surface detector [9], independent of energy above 3 EeV. At this energy, which is the lower bound for the derived surface detector spectrum, all the air-showers trigger at least 3 stations and can be reconstructed. This simple selection criteria makes the acceptance free of MC assumptions, as it does not depend on the reconstruction. The energy resolution and the bias due to signals upward fluctuations (about 20% at the lowest energies with a positive bias of 5% and about 7% with no bias at the highest energies) modify, through bin-to-bin migrations in a steep falling distribution, the flux and the spectral shape. To correct for these effects a forward folding procedure is applied, using an energy migration matrix obtained from MC simulations of the air-showers and of the detector response. The correction factor

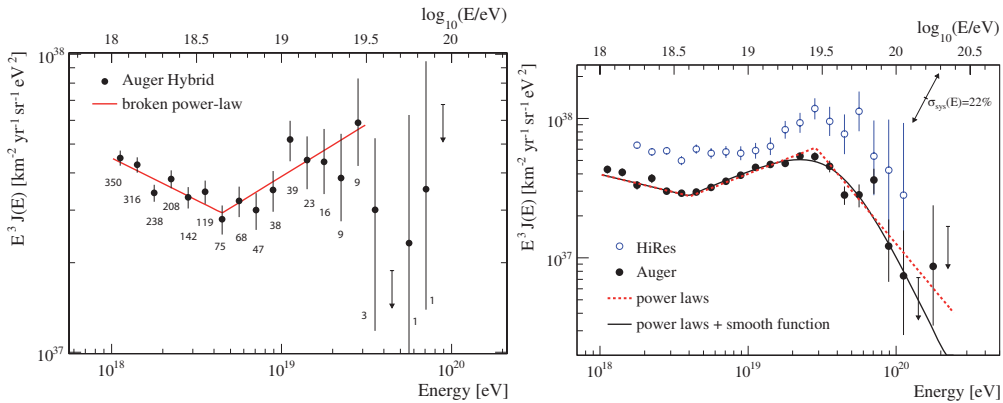


Fig. 2. – (Left) The energy spectrum of the highest energy cosmic rays obtained from hybrid measurements. Only statistical uncertainties are shown. The numbers correspond to the amount of events in each energy bin. (Right) The Auger energy spectrum, fitted with a broken power law function in the ankle region and a soft Fermi-like transition at the highest energies. The HiRes spectrum, illustrated with open symbols, is compatible with the Auger spectrum within the energy systematic uncertainties.

that is applied to the flux, less than 20%, is obtained from a simple flux parametrisation which, folded with the migration, describes best the raw data.

The systematic uncertainties that are inherited from the mass composition and the energy conversion assumed in the MC samples are about 5% over the whole energy range. This, together with the systematic uncertainties on the acceptance (3%) lead to a 6% uncertainty of the flux.

The hybrid events allow to extend the energy spectrum up to 1 EeV in the region of the ankle. The hybrid exposure calculation relies on an accurate simulation of the fluorescence detector and of the atmosphere. A large sample of Monte Carlo simulations is performed to reproduce the exact conditions of the experiment and the entire sequence of given configurations, from camera pixels to the combined SD-FD data taking of the observatory. The rapidly growing array, as well as the seasonal and instrumental effects, are reproduced in the simulations within 10 min time intervals. The systematic uncertainty in the hybrid spectrum is currently dominated by the calculation of the exposure and reaches 10% at 1 EeV and 6% at 10 EeV. The energy spectrum obtained from the hybrid events is illustrated in the left panel of fig. 2 together with the number of events in each energy bin.

The energy calibration of the surface detector data is done with the fluorescence detector events, therefore the systematic uncertainty on energy is common for both data sets and is at a level of 22%. The largest contribution is given by the fluorescence yield measurements (14%) and from the detector calibrations (9.5%). The energy spectra obtained with the surface detector and with the hybrid detector are combined using a maximum likelihood method. The Auger energy spectrum, scaled with E^3 is shown in fig. 2 in the right panel. The presence of a change in the energy spectrum at $\log_{10}(E/\text{eV}) = 18.61 \pm 0.01$, the ankle, is observed, a continuation of the same power law as above the ankle can be rejected with more than 20σ .

The events in the flux suppression energy region have shown a strong correlation with the Veron-Cetty and Cetty catalogue in 3.1° angular distance and within 75 Mpc [10].

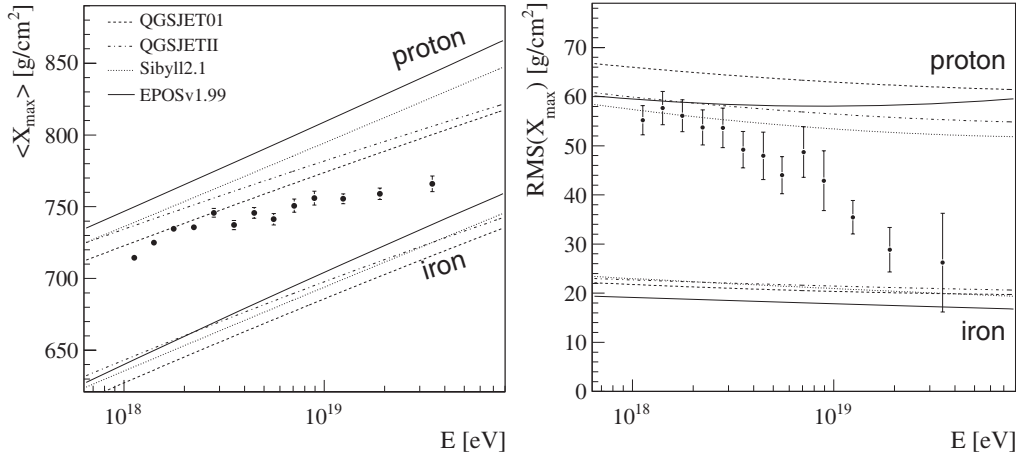


Fig. 3. – The mean (left) and the RMS (right) of the shower maximum as a function of energy. The predictions for proton and iron compositions of different high energy hadronic interaction models are illustrated [11].

The updated data taken after the anisotropy establishment still show a correlation, but weaker than the initial data set [12]. Based on *a posteriori* analysis, an excess of events is also observed from a region of the sky close to Cen A. Larger statistics is still needed to identify the sources of ultra high energy cosmic rays.

4. – Mass composition

4.1. Energy dependence. – The maximum of the shower development (X_{\max}) and its fluctuations are parameters that are sensitive to the mass of the primary particles. The average of X_{\max} , $\langle X_{\max} \rangle$, in a simple Heitler model depends linearly on the logarithm of energy for the same primary and is also a linear function of the mean logarithm of the primary mass. Therefore a change in the elongation rate, *i.e.* the rate of change of $\langle X_{\max} \rangle$ per logarithm of energy can be used to study relative changes in the composition. The shower-to-shower fluctuations of X_{\max} are related to the primary cross section with air and decrease with the number of nucleons.

The measured $\langle X_{\max} \rangle$ and the $\text{RMS}(X_{\max})$ as a function of energy [11] are illustrated in fig. 3. The predictions from air-shower simulations are represented by lines. The achieved resolution on X_{\max} is 20 g/cm^2 above a few EeV. This has been determined both from simulations and from independent measurements of the same shower with two FD stations. The systematic uncertainties from the calibration, atmospheric conditions, reconstruction and event selection on the average X_{\max} are less than 13 g/cm^2 and less than 6 g/cm^2 for the $\text{RMS}(X_{\max})$.

As can be seen from fig. 3, a decrease of the fluctuations from 55 to 26 g/cm^2 with increasing energy is observed as well as a change in the elongation rate at $\log_{10}(E/\text{eV}) = 18.24 \pm 0.05$ from $(106^{+35}_{-21}) \text{ g/cm}^2/\text{decade}$ to $(24 \pm 3) \text{ g/cm}^2/\text{decade}$. This energy coincides approximately with the energy of the ankle determined in the energy spectrum.

On the assumption that the hadronic interactions properties do not change drastically in the energy range of interest, the evolution with energy can be interpreted as an increase of the average mass of cosmic rays. The differences between different high energy

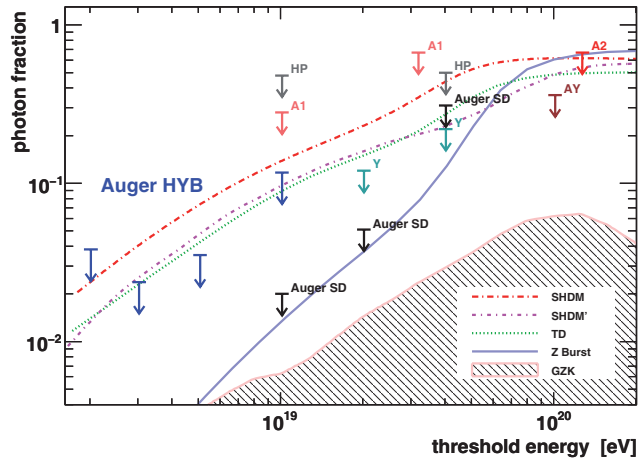


Fig. 4. – Upper limits on the photon fraction in the integral cosmic-ray flux (95% CL) as derived from the data of the surface detector (Auger SD) at highest energies and the limits above 2, 3, 5, and 10 EeV as obtained with the fluorescence detector (Auger Hyb). The shaded region represents the expected GZK photon fraction, while by lines are indicated predictions from top-down models [13].

hadronic interaction models is large and the current models do not cover the whole possible extrapolations of lower energy accelerator data. Within the current model predictions a transition from light to heavy composition is supported.

4.2. Photons and neutrino limits. – The detection of neutrino of ultra high energy would open a new window in the cosmic rays physics, mostly because they would point directly to their sources, being undeflected by the magnetic fields and not interacting with the traversed extraterrestrial matter. At the production sites of hadronic cosmic rays neutrino and photon fluxes are produced and also through the GZK effect photons and neutrinos would result from the secondary pions from the interaction of the cosmic rays with the infrared light or with the CMB.

For the production of UHECRs there exist numerous *top-down* scenarios. In these cases the cosmic rays are originating from decays of meta-stable heavy particles like super-heavy dark matter, topological defects collapses, or from interactions of neutrino with the relic neutrino background. One of the common features for these models is that they predict high fluxes for photons and neutrinos.

A clear signature for photons is the deep X_{\max} . Photon cross section is suppressed by the LPM effect, therefore the first interaction is much deeper in the atmosphere than for protons and also the multiplicity of the secondaries is lower. The shower cascades are mainly produced through electromagnetic processes therefore the particle content on the ground is muon poor. The maximum of the shower development is used in case of the hybrid data and the electromagnetic-like footprint on the ground in the case of the surface detector [13]. The resultant 95% CL upper limits on the photon fractions in the EeV region measured with the hybrid data, are 3.8%, 2.4%, 3.5% and 11.7% for the primary energies above 2, 3, 5 and 10 EeV, respectively, and are illustrated fig. 4. These limits together with the ones derived from the surface detector dismiss or disfavour the *top-down* scenarios.

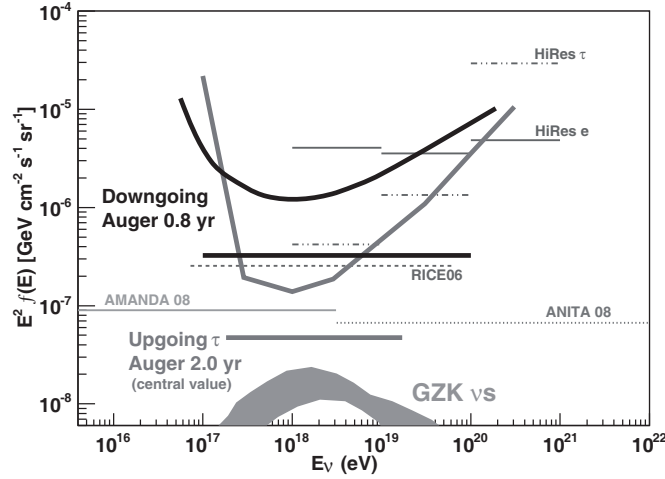


Fig. 5. – Integrated and differential upper limits for single flavour of diffuse neutrino fluxes (90% CL) for up-going ν_τ and down-going ν . The shaded region represents the expected GZK neutrino flux [12].

The neutrinos can be observed at the Auger site [14,12] by their specific signatures as almost horizontal (down-going) or up-going air-showers in an early stage of development. For up-going ν the search is performed in the hypothesis that the tau neutrinos interact in the Earth and produce tau leptons which generate air-showers in the lower part of the atmosphere. An end-to-end chain is simulated, from the earth skimming neutrinos, the extensive air showers in the atmosphere to the detector response to calculate exposure and their discrimination power. The systematic uncertainties at low energies are dominated by the contributions from the τ polarisation ($^{+17\%}_{-10\%}$), the ν cross-section ($^{+5\%}_{-9\%}$) and the τ energy losses ($^{+25\%}_{-10\%}$), while at high energies the contributions from the topography at the site, and from the MC simulations of air-showers and of the detector ($^{+20\%}_{-5\%}$) are prominent. In the period 1 Nov 2007-28 Feb 2009 no down-going ν were observed and in the period 01 Jan 2004-28 Feb 2009 no up-going ν_τ were identified. The differential and integrated limits are shown in fig. 5.

Conclusions

The measurements at the Pierre Auger Observatory, containing data equivalent to 2 years of fully operational experiment, indicate a change in the nature of cosmic rays at around 3 EeV and show a change in the shape of the energy spectrum and the elongation rate. These measurements add support to the hypothesis that an extragalactic component of mixed composition starts to dominate in this energy range. The near-future particle accelerator results will constrain the hadronic interaction models and the interpretation of the evolution of the shower maximum with energy will be more conclusive.

The photon limits exclude most of the top-down scenarios above 2 EeV. In the next 20 years of operation the photon fraction measurement will be sensitive to a level of less than 0.1% and the neutrino limits, if no neutrino is observed, will improve by more than an order of magnitude. These determinations, together with the arrival directions and mass composition analysis will help solving the origin of the highest energy cosmic rays.

REFERENCES

- [1] GREISEN K., *Phys. Rev. Lett.*, **16** (1966) 748.
- [2] ZATSEPIN G. T. and KUZ'MIN V. A., *JETP Lett.*, **4** (1966) 78.
- [3] HILLAS A. M., to be published in *Phys. Rev. Lett.*; BEREZINSKY V. S. and GRIGOREVA I. S., *Astron. Astropart.*, **199** (1988) 1; ALLARD D., PARIZOT E. and OLINTO A. V., *Astropart. Phys.*, **27** (2007) 61.
- [4] PIERRE AUGER COLLABORATION, *Nucl. Instrum. Methods A*, **523** (2004) 50.
- [5] PIERRE AUGER COLLABORATION, *Nucl. Instrum. Methods A*, **568** (2006) 839.
- [6] PIERRE AUGER COLLABORATION, *Proc. 31st ICRC, Lodz, 2009*; arXiv:0908.4422.
- [7] PIERRE AUGER COLLABORATION, arXiv:0710.1646.
- [8] UNGER M. *et al.*, *Nucl. Instrum. Methods A*, **588** (2008) 433.
- [9] PIERRE AUGER COLLABORATION, *Nucl. Instrum. Methods A*, **613** (2010) 29.
- [10] PIERRE AUGER COLLABORATION, *Astropart. Phys.*, **29** (2008) 188; *Science*, **318** (2007) 939.
- [11] PIERRE AUGER COLLABORATION, *Phys. Rev. Lett.*, **104** (2010) 091101.
- [12] PIERRE AUGER COLLABORATION, *Proc. 31st ICRC, Lodz, 2009*; arXiv:0906.2347.
- [13] PIERRE AUGER COLLABORATION, *Astropart. Phys.*, **31** (2009) 399; **29** (2008) 188.
- [14] PIERRE AUGER COLLABORATION, *Phys. Rev. D*, **79** (2009) 102001.